Electronic Supplementary Material (ESI) for Journal of Materials Chemistry A.

A recrystallized organic cathode with high electrical conductivity for fast sodium-ion storage

Zixuan Shan ‡,[a] Shuangqin Yang ‡,[a] Xinya Zhang,[a] Yuan Chen*[a]

[a]College of Energy Materials and Chemistry, Inner Mongolia University, Hohhot, 010070, China

‡ These authors contributed equally.

* Corresponding authors.

E-mail addresses: yuanchen@imu.edu.cn

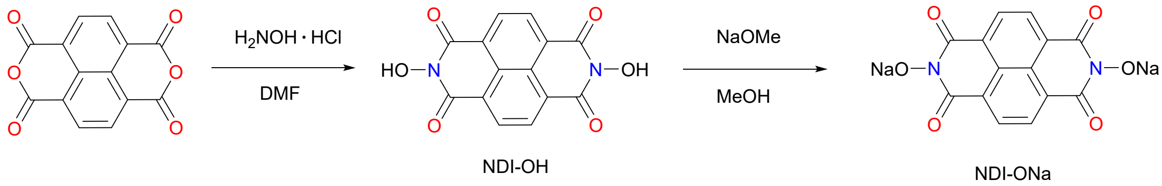

Figure S1. Schematic of the synthesis of NDI-ONa.

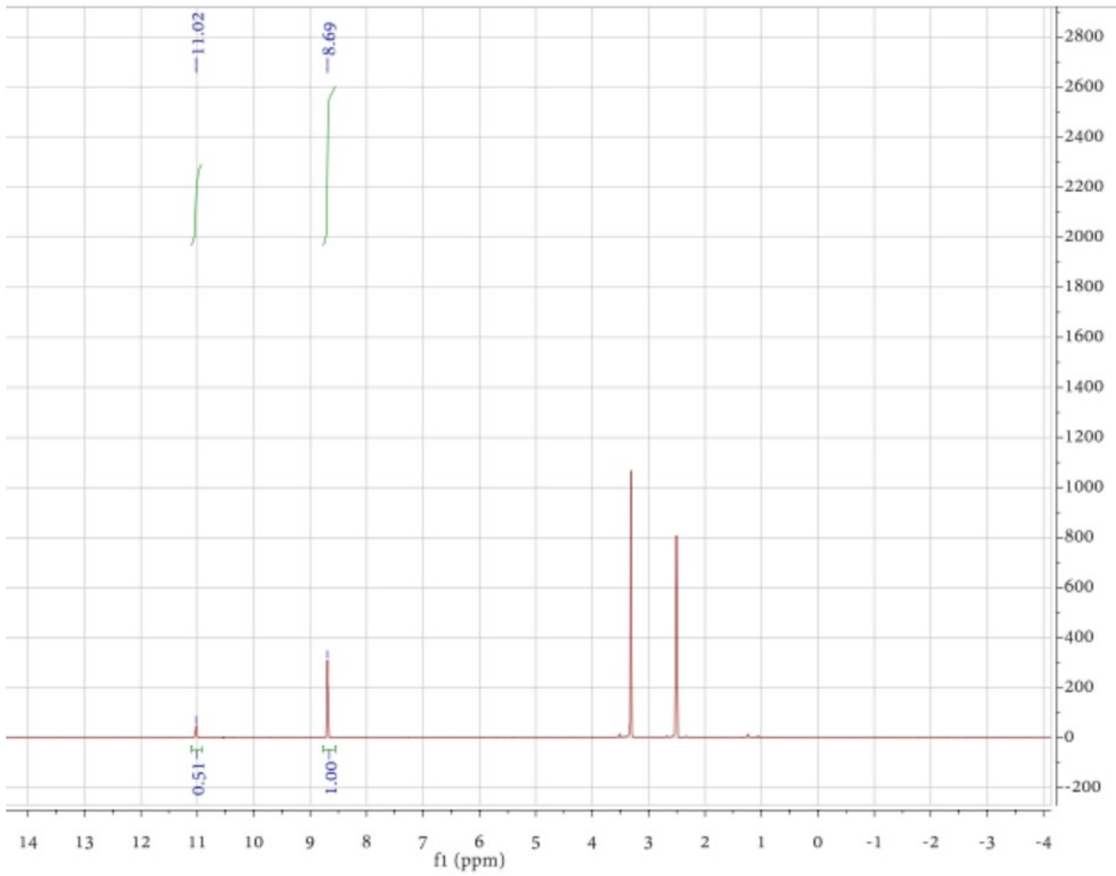

Figure S2. ^{1}H-NMR spectrum of the NDI-OH.

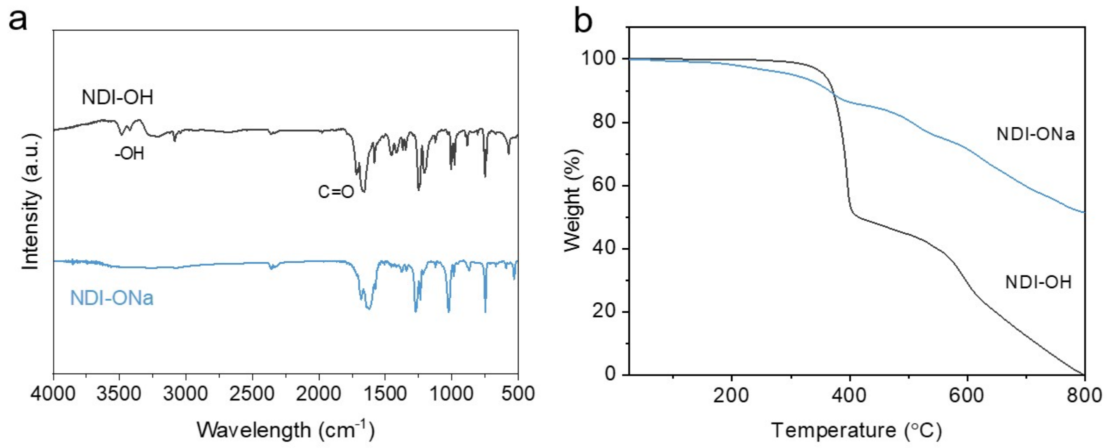

Figure S3. (a) the FTIR spectra, (b) TGA curves of NDI-OH and NDI-ONa, respectively.

Table S1. EA of NDI-OH and NDI-ONa.

		C%	N%	H%	O%	Na%
NDI-OH	Calculated	56.39	9.39	2.03	32.19	-
($C_{14}H_6N_2O_6$)	Found	56.05	9.25	1.88	32.45	-
NDI-ONa	Calculated	49.14	8.19	1.18	28.05	13.44
($C_{14}H_4N_2O_6Na_2$)	Found	48.45	8.75	1.78	28.85	14.12

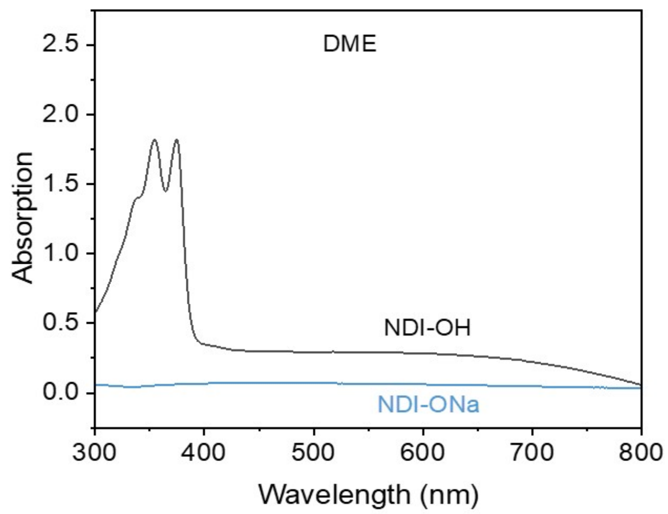

Figure S4. UV spectra of NDI-OH and NDI-ONa in DME. After salinization, the NDI-ONa showed insoluble in DME solvent.

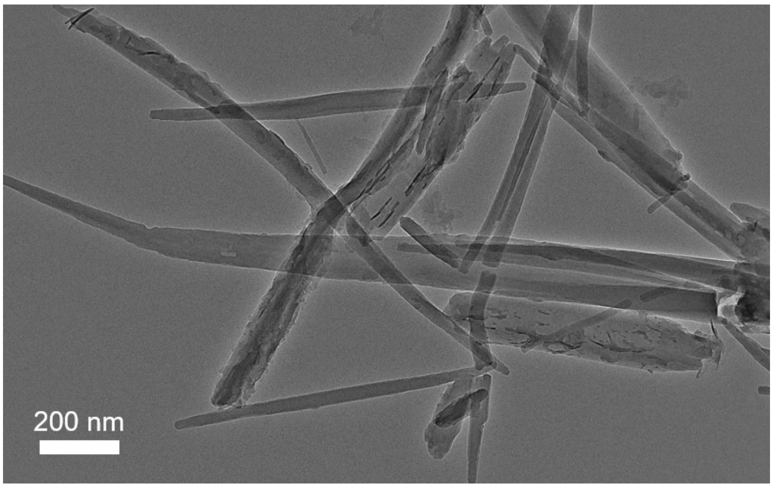

Figure S5. TEM image of NDI-ONa-r.

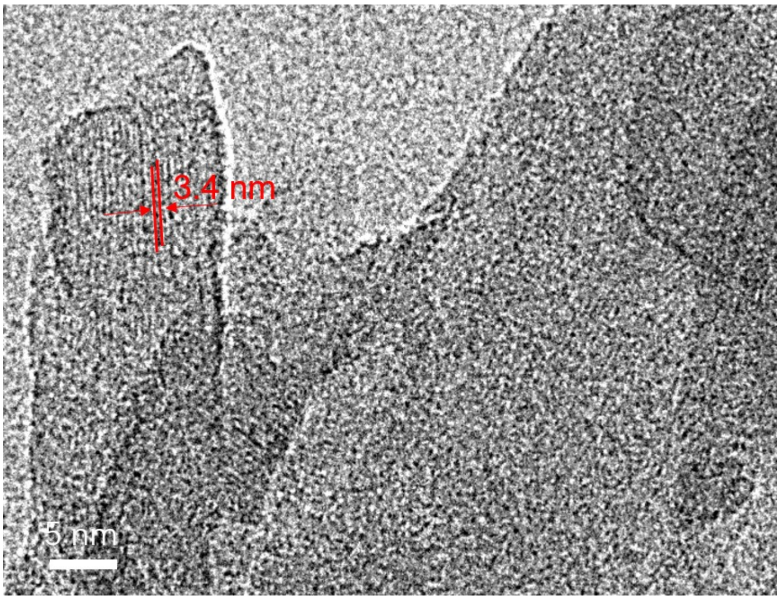

Figure S6. HR-TEM image of NDI-ONa-r.

Table S2. Electrical conductivity of NDI-OH and NDI-ONa

	R (Ω)	*d* (mm)	σ (S m^{-1})
NDI-OH	2.7×10^{9}	0.29	8.1×10^{-10}
NDI-ONa-p	3.05×10^{7}	0.27	6.7×10^{-8}
NDI-ONa-r	1.14×10^{6}	0.26	1.7×10^{-6}

The electronic conductivity was calculated according to the following equation:

$$\sigma = \frac{d}{RS}$$

where R, S, d are resistance value, area (1.33 cm^{-2}) and thickness of the pellet, respectively.

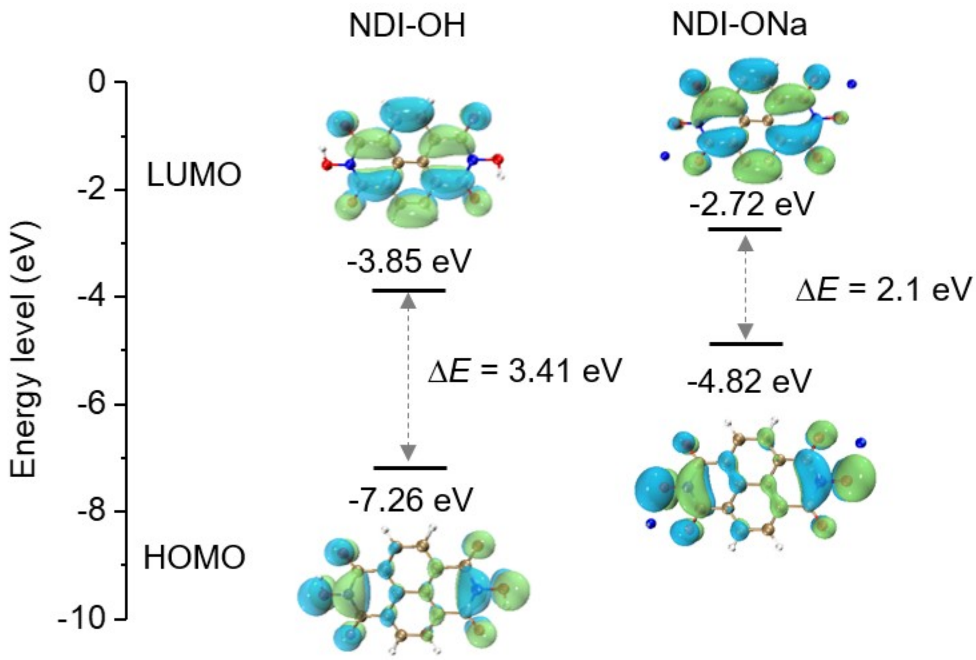

Figure S7. Calculated HOMO and LUMO energy levels of NDI-OH and NDI-ONa.

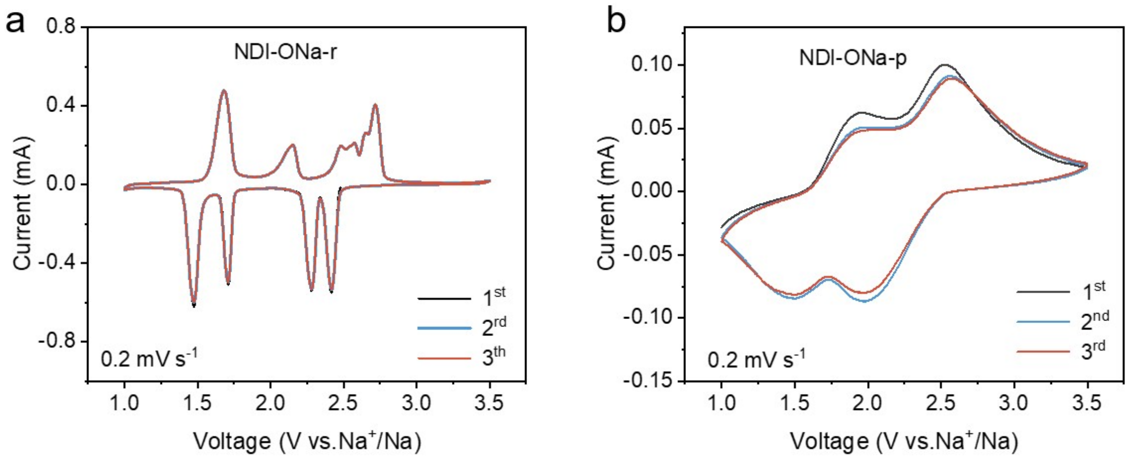

Figure S8. The CV curves of (a) NDI-ONa-r and (b) NDI-ONa-p at 0.2 mV s^{-1}, respectively.

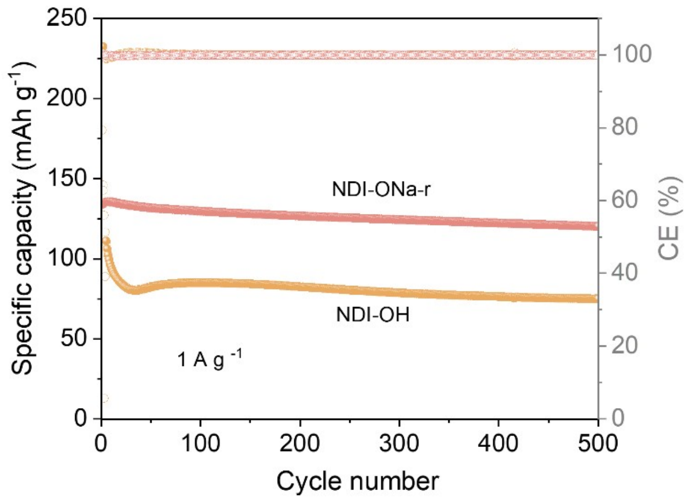

Figure S9. The cycling performances of NDI-ONa-r and NDI-OH at 1 A g^{-1}.

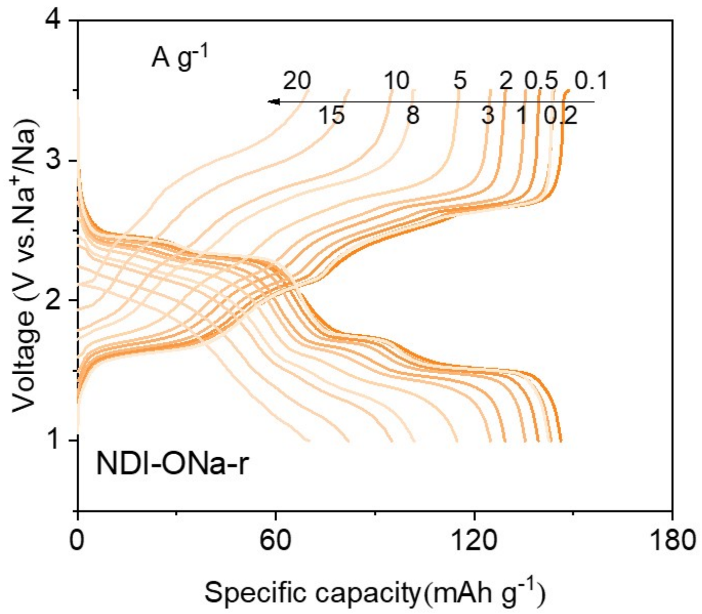

Figure S10. The discharge and charge profiles of NDI-ONa-r at different current densities.

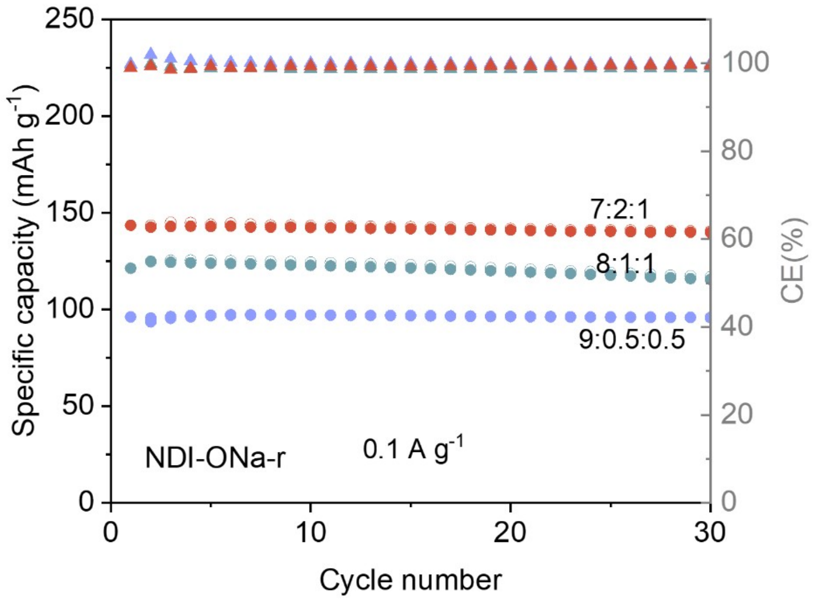

Figure S11. Comparisons of the capacity with three ratios of active materials.

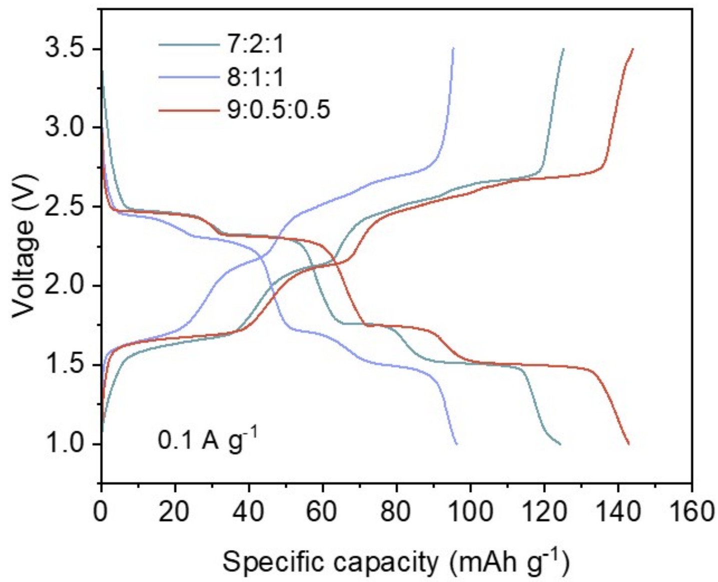

Figure S12. The discharge and charge profiles of NDI-ONa-r with three ratios of active materials.

Table S3. The equivalent circuit and the values of the electrical elements of the NDI-ONa-r and NDI-ONa-p in different states.

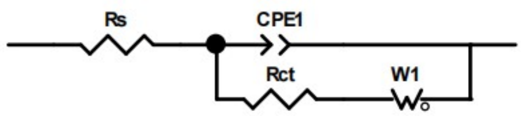

Rct (Ω)	Pristine	1^{st}	3^{nd}
NDI-ONa-r	4.044	9.439	10.25
NDI-ONa-p	477.6	536.8	661.3

Rs, CPE1, Rct and W1 represent the ohmic resistance, constant phase element, charge-transfer resistance and Warburg resistance, respectively.

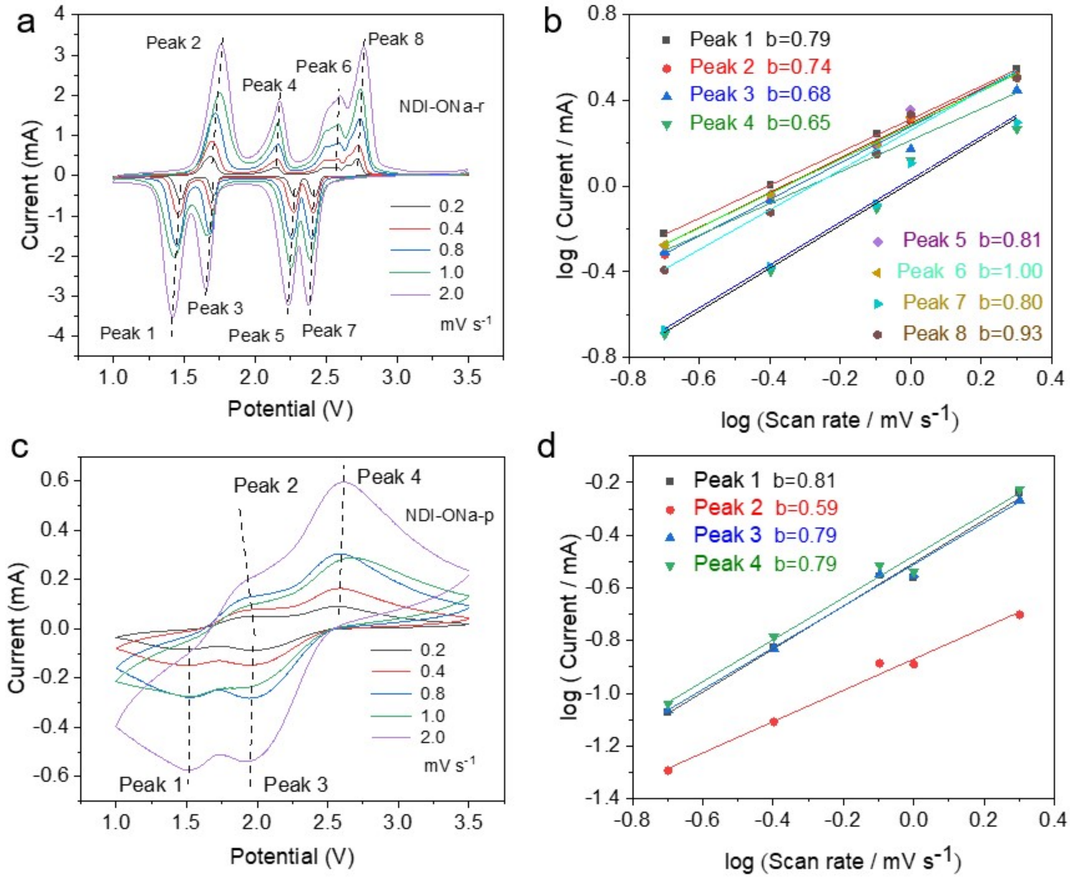

Figure S13. (a, c) CV curves of NDI-ONa-r and NDI-ONa-p at various scan rates. (b, d) The linear fits of log(i) vs. log(v) plots.

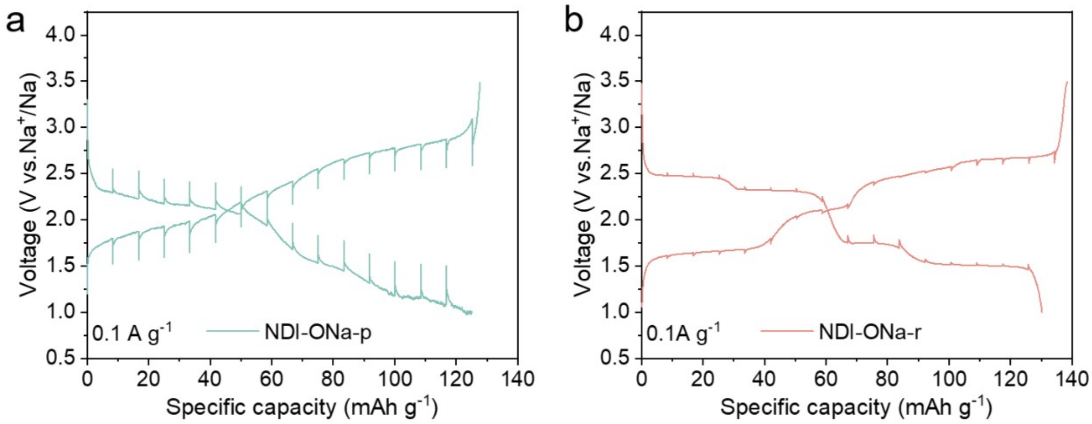

Figure S14. The GITT curves of (a) NDI-ONa-p and (b) NDI-ONa-r cathodes at 0.1 A g^{-1}, respectively.

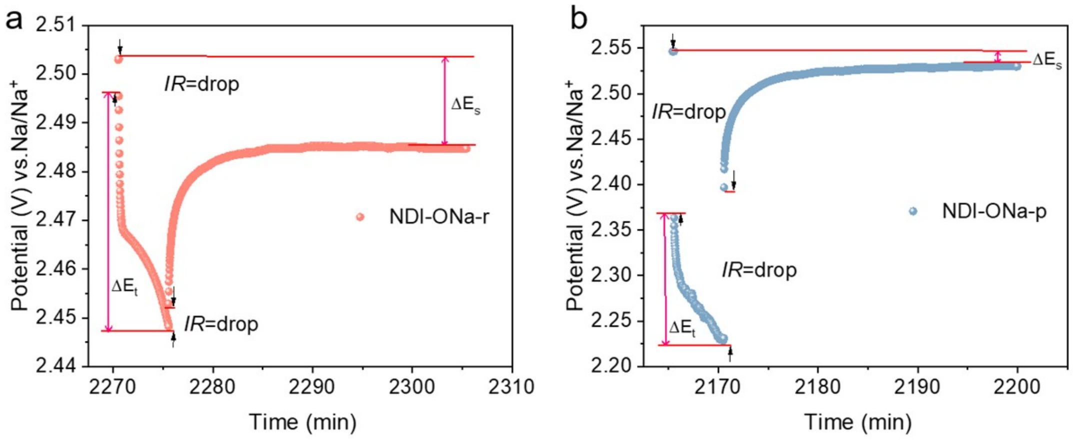

Figure S15. GITT potential response curve with time for one typical discharge step of (a) NDI-Oa-r and (b) NDI-ONa-p, respectively. The lower IR values also further indicated that NDI-ONa-r exhibited faster electrochemical reaction kinetics.

The Na^+ ion diffusion coefficient (D_{Na+}) was further calculated by according to the following equation:

$$D_{Na+} = (4/\pi\tau)\times({}^{m_B V_M}/{}_{M_B S})^2\times({}^{\Delta E_s}/{}_{\Delta E_t})^2$$

where τ is the time of current pulse, and m_B, V_M, M_B, and S are the mass loading, molar volume, molar mass and electrode-electrolyte interface area of the material, respectively. ΔE_s is the voltage difference between the initial state and the steady state of each step, and ΔE_t is the voltage change resulting from the current pulse excluding the IR drop.

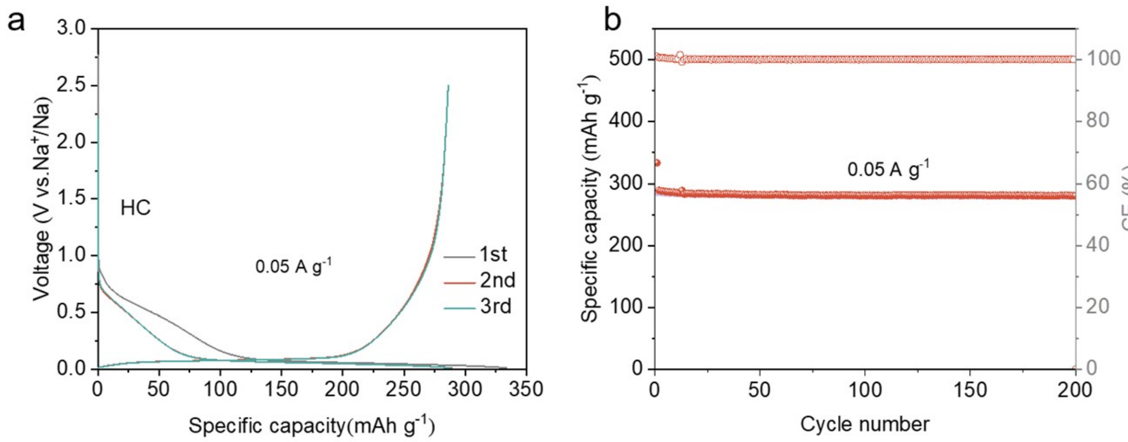

Figure S16. (a) The discharge and charge profiles and (b) cycling performance at 0.05 A g^{-1} of HC anode.

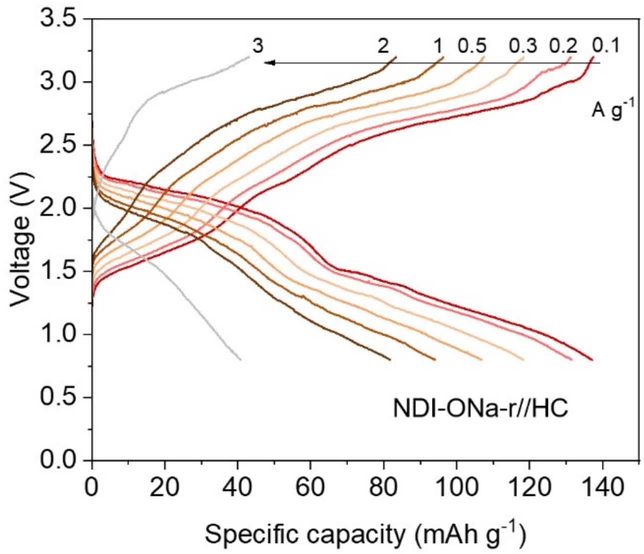

Figure S17. Charge-discharge curves of NDI-ONa-r//HC full cell at different densities.

Table S4. Comparison of NDI-ONa-r cathode and the organic cathode materials reported in the literature for SIBs.

Materials (reference)	Electrode composition	Specific capacity (mAh g^{-1}) (Current density, A g^{-1})	Cycle Stability Retention/ Cycles/ Current density	Ref.
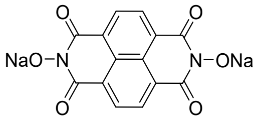 NDI-ONa-r	7:2:1	145 (0.1) 70 (20)	87%, 30000, 10A g^{-1}	**This work**
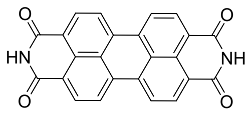 PTCDI	7:2:1	138 (0.02) 103 (0.6)	90%, 300, 0.2 A g^{-1}	*ACS Appl. Mater. Interfaces* 2015, 7, 21095
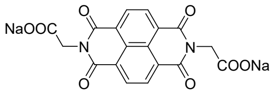 Na_2BNDI	6:3:1	111 (0.1 C) 77 (50C)	57.3%, 70000, 10C	*Adv. Energy Mater*. 2021, 11, 2101972
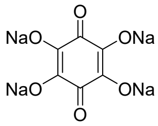 $Na_4C_6O_6$	7:2:1	170 (0.5)	71.9%, 1000, 0.1 A g^{-1}	*J. Am. Chem. Soc*. 2024, *146*, 1619-1626
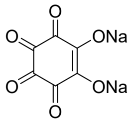 $Na_2C_6O_6$	7:2:1	205 (0.02) 102 (1)	75%, 500, 0.05 A g^{-1}	*Chem* 2017, *3*, 1050
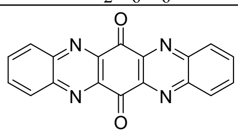 TAPQ	7:2:1	257 (0.1) 236 (5)	72%, 1000, 1 A g^{-1}	*Angew. Chem. Int. Ed*. 2021, *60*, 26806-26812
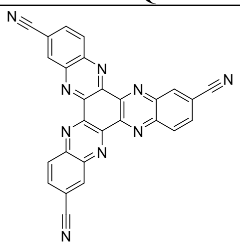 3CN-DPZ	7:2:1	80.9 (2) 64.3 (12)	97.9%, 5000, 64 A g^{-1}	*Chem. Eng. J*. 2023, 451, 138652
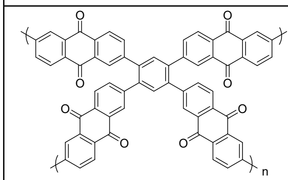 PABQ-3	6:3:1	193 (0.1) 150 (10) 101 (40)	95.8%, 1000, 0.05 A g^{-1}	*ACS Nano* 2022, *16*, 14590
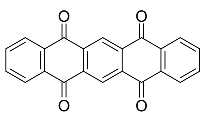	70:15:10:5	129 (0.05) 75 (1) 11 (5)	63%, 300, 0.05 A g^{-1}	*Adv. Mater.* 2016, 28, 9182

PT				
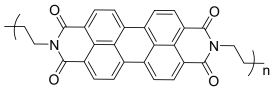 PI2	6:3:1	137 (0.2 C) 75 (5 C)	86%, 5000, 0.8C	*Adv. Energy Mater*. 2014, *4*, 1301651
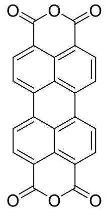 PTCDA	6:3:1	126 (0.2) 99 (5)	94%, 400, 1 A g^{-1}	*Energy Storage Materials*, 2022, 61-68
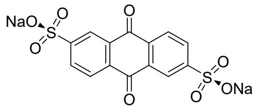 $Na_2AQ26DS$	active materials: KB:CNTs:La133:PVDF=70:10:10:7:3	87 (0.5) 30 (5)	72%, 1000, 0.5 A g^{-1}	*ChemSusChem* 2020, *13*, 1991-1996
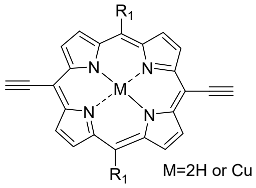 PTO	85:5:10	172 (0.2) 138 (10)	93%, 600, 5 A g^{-1}	*Nano-Micro Lett.* 2021, *13*, 71
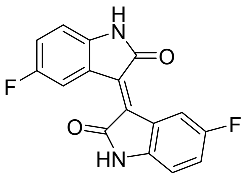 EFID	7:2:1	135 (0.1) 28 (5)	91.2%, 2000, 0.2 A g^{-1}	*Adv. Sci.* 2024, *11*, 2307134
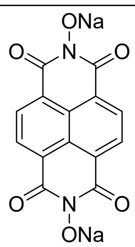 NDI-ONa	6:3:1	170 (0.1) 159 (2)	93%, 20000, 3A g^{-1}	*ACS Nano* 2023, *17*, 21432-21442
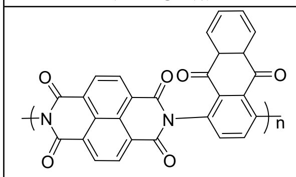 PAQI	4:4:2	200 (0.05) 60 (1)	93%, 150, 0.05 A g^{-1}	*J. Mater. Chem. A 2016, 4, 11491-11497*
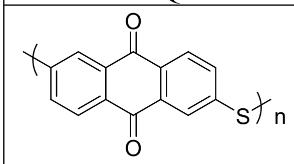 PAQS	6:3:1	175 (0.05) 110 (1)	-	*Adv. Energy Mater. 2020, 10, 2002780*
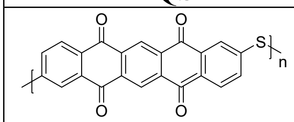 PPTS	4:5:1	290 (0.1) 170 (10)	86%, 5000, 10 A g^{-1}	*Chem 2018, 4, 2600-2614*

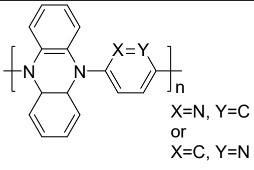 BPyPz	7:2:1	205 (0.5) 126 (20)	89%, 300, 0.5 Ag^{-1}	*J. Mater. Chem. A*, 2023, *11*, 2711
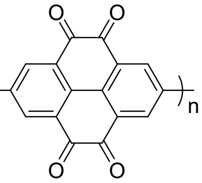 PPTO	8:1:1	287.6 (0.1) 216.6 (5.0)	95.1%, 1300, 10 A g^{-1}	*Adv. Energy Mater*. 2020, 11, 2002917